Remnant High Density Lipoprotein$_2$ Particles Produced by Hepatic Lipase Display High-Affinity Binding and Increased Endocytosis into a Human Hepatoma Cell Line (HEPG$_2$)[†]

Karim Guendouzi, Xavier Collet, Bertrand Perret, Hugues Chap, and Ronald Barbaras*

Institut National de la santé et de la Recherche Médicale (INSERM) - Unité 326, Hopital Purpan, 31059, Toulouse, France

Received May 6, 1998; Revised Manuscript Received August 12, 1998

ABSTRACT: We had previously shown that hepatic lipase plays a prominent role in promoting the generation of pre-β HDL particles from triglyceride rich HDL$_2$, leaving an α-HDL particle of decreased size that was named "remnant HDL$_2$" [Barrans, A., et al. (1994) *J. Biol. Chem. 269*, 11572−11577]. Interestingly, this remnant HDL$_2$ was rapidly cleared by the liver, suggesting a particularly high affinity of those remnant HDL$_2$ for liver cells. In the present study, we attempted to characterize the interaction of remnant HDL$_2$ with HepG$_2$ cells, as compared to those of native triglyceride rich HDL$_2$. Two main observations were made. First, while triglyceride rich HDL$_2$ particles were able to bind only the low-affinity binding sites, the remaining particle generated after hepatic lipase lipolysis the remnant HDL$_2$ was further able to bind to the high-affinity binding sites. Competition experiments indicate that these two remnant HDL$_2$ binding sites were the same as the two HDL$_3$ binding sites previously described [Barbaras, R., et al. (1994) *Biochemistry 33*, 2335−2340]. This is the first observation on the remodeling dependence of HDL binding onto hepatocytes. Second, following binding on those two binding sites, the remnant HDL$_2$ were faster internalized and in higher amounts than the native triglyceride rich HDL$_2$. All together, these observations suggest that the continuous remodeling of HDL induces different binding and internalization characteristics of the HDL particles and that the high-affinity HDL binding sites might trigger the internalization of apo HDL through the low-affinity binding sites.

The levels of plasma high-density lipoprotein (HDL)[1] are inversely correlated to the incidence of atherosclerosis and coronary artery disease (*1*). The protective effect of the HDL involves the reverse transport of cholesterol from peripheral cells to the liver (*2*). It appears likely that a number of different cellular mechanisms, possibly receptor dependent and independent, are required to regulate this pathway. Moreover, in the vascular compartment, HDL particles undergo continuous remodeling, and thus, the HDL subspecies which specifically interact with hepatocytes, for instance, are not clearly defined. At this time, HDL$_2$ represents the best candidate in the removal of the large HDL particles by the liver. In a previous study, we have demonstrated in our group the existence of two classes of HDL-binding sites on a human hepatocyte cell line (HepG$_2$). Furthermore, if the low-affinity binding sites seem to be responsible for the apo-HDL internalization, the role of the high-affinity binding site remains to be elucidated (*3, 4*). In parallel, we had previously shown that hepatic lipase plays a prominent role in promoting the generation of pre-β HDL particles from triglyceride rich HDL$_2$, leaving an α-HDL particle of decreased size that was named "remnant HDL$_2$" (*5*). Interestingly, this remnant HDL$_2$ was rapidly cleared by the liver, suggesting a particularly high affinity of those remnant HDL$_2$ for liver cells. In an attempt to identify the mechanism by which remnant HDL$_2$ was removed by the liver, the high- and low-affinity sites of these particles were in vitro studied with HepG$_2$ cells and compared to their counterparts, which were not treated by hepatic lipase. The internalization and degradation of these particles were also studied.

EXPERIMENTAL METHODS

Materials. Bovine serum albumin (BSA) was obtained from Sigma (La Verpilliere, France). [^{125}I]Na was from Amersham (France). All cell culture reagents were from Life Technologies (France). All other reagents used were of an analytical grade.

Cells. The human hepatoblastoma-derived cell line HepG$_2$ was obtained from the American Type Culture Collection (Rockville, MD). Cells were plated at (1−2) × 10^4 cells/well in 48 multiwell plates (Falcon) for binding, competition, and kinetic assays and 24 multiwell plates for internalization assays (4 × 10^4 cells/well). Cells were grown in Dulbecco's modified Eagles medium supplemented with 10% fetal calf serum, 100 units/mL penicillin, and 100 μg/mL streptomycin at 37 °C in a 5% CO_2 and 95% air incubator. Medium was changed every 2 or 3 days, and the cells were subcultured every 7−8 days.

[†] This work was supported in part by a research grant from ARCOL.

* To whom correspondence should be addressed. Tel: (33) 5 61 77 94 14. Fax: (33) 5 61 77 94 01. E-mail: Ronald.Barbaras@purpan.inserm.fr.

[1] Abbreviations: HDL, high-density lipoprotein; TG rich-HDL$_2$, triglyceride rich-high-density lipoprotein; LDL, low-density lipoprotein; oxLDL, oxidized LDL; acLDL, acetylated LDL; VLDL, very low-density lipoprotein; CLA-1, CD36 and LIMPII analogous protein-1; CETP, cholesterol ester transfer protein; HL, hepatic lipase; SDS, sodium dodecyl sulfate; PBS, phosphate buffer saline; TCA, trichloroacetic acid.

10.1021/bi9810508 CCC: $15.00
Published on Web 10/02/1998

Lipoprotein Preparation. High-density lipoproteins (HDL_3 and HDL_2) were isolated from the plasma of normolipidemic healthy human donors. Disodium ethylenediaminetetraacetic acid (Na_2EDTA) and sodium azide were added to final concentrations of 1 mM and 0.05% (w/v), respectively. The lipoproteins were obtained by sequential flotation ultracentrifugation. After washing at their lower density limit (1.07 g/mL), total HDL were isolated (1.085−1.19 g/mL) and further fractionated at $d = 1.125$ g/mL into HDL_2 and HDL_3.

HDL_2 were enriched in triacylglycerol by incubation at 37 °C during 6 h in the presence of very low-density lipoprotein (VLDL) and the lipoprotein-deficient fraction ($d > 1.25$ g/mL), as a source of cholesterol ester transfer protein (CETP). After removing VLDL at $d = 1.07$ g/mL, triglyceride rich HDL_2 were reisolated by ultracentrifugation at 1.21 g/mL. Modified HDL_2 were dialized and were then incubated with or without partially purified hepatic lipase in the presence of free fatty acid albumin, during 2 h at 37 °C as previously described (*5*). Immediately after, triglyceride rich HDL_2 and remnant HDL_2 were isolated by ultracentrifugation at 1.19 g/mL.

^{125}I-Labeling of HDL_3, triglyceride rich HDL_2, and remnant HDL_2 was performed by the *N*-bromosuccinimide method according to Sinn et al. (*6*). Specific radioactivity ranged 1000−3000 cpm/ng of protein.

Binding Assays. Binding of labeled lipoproteins to $HepG_2$ cells was performed for 1.5 h at 4 °C as previously described (*4*). Briefly, cell monolayers were incubated in phosphate-buffered saline (PBS) with increasing concentrations of labeled ligands and were then washed with ice-cold PBS (maximum washing time was 15 s). To determine the cell-associated radioactivity, 500 μL of 0.1 N NaOH was added to the washed monolayer. The NaOH digest was used for radioactivity measurement and protein determination. Nonspecific binding was determined in the presence of a 100-fold excess (compared to the K_d value) of unlabeled HDL_3. The value of nonspecific binding varied from 30 to 40% of total binding. The ratio of bound to free [^{125}I]apo-HDL versus bound ^{125}I-labeled apo-HDL was plotted according to Scatchard (*7*).

Competition Assays. As for the binding, the competition assays were performed at 4 °C for 1.5 h. A concentration of 10 μg/mL ^{125}I-labeled HDL_3 was used, and increasing concentrations of unlabeled competitors were added. Washing and radioactivity were performed as above. Data were expressed as the percent of the specific binding, measured in the absence of competitor, versus the log of lipoprotein concentration (in micrograms of protein per milliliter).

Kinetic Assays. The association rate constant (k_{+1}) of different ligands was determined by measuring the amount of protein specifically bound to $HepG_2$ cells at 4 °C and at different times. The concentration of ^{125}I-labeled lipoprotein was constant during all experiments (75 μg/mL). The determination of nonspecific binding and all the washing and radioactivity measurements were performed as for binding assays. A pseudo-first-order method was used for k_{+1} calculation as previously described (*4*). Dissociation experiments were carried out on $HepG_2$ cells at 4 °C using 75 μg/mL of labeled ligand. After the association equilibrium binding was reached (i.e., 90 min) and after two washes in ice-cold PBS, fresh medium was added to the cells. Under these conditions, we can use a first-order equation to calculated k_{-1}. Thus, a plot of $\ln(B/B_o)$ versus time (where B_o is the binding value at time = 0, i.e., at equilibrium) will have a slope of $-k_{-1}$. Alternatively, k_{-1} can be estimated as $k_{-1} = 0.693/t_{1/2}$, where $t_{1/2}$ is the time when $B = 0.5B_o$ (*8*).

Internalization Assays. Internalization of labeled lipoproteins was performed at 37 °C as previously described (*3*). Cells were incubated in PBS with labeled ligands during 90 min, then washed twice with ice-cold PBS. Depletion of labeled ligands present on the cell surface was performed at 4 °C for 90 min with PBS. Radioactivity was measured as for binding assays. At 37 °C, before depletion, the cell associated radioactivity is referred to as "binding + internalization". For each experiment, the internalization was determined by measuring the cell-associated radioactivity remaining after depletion in PBS at 4 °C. Nonspecific internalization was determined in the presence of an excess of HDL_3 and varied from 30 to 40% of the total internalization.

^{125}I-Labeled lipoprotein degradation was assessed, after internalization, by measuring the trichloroacetic acid (TCA) nonprecipitable material present in the cells after a slight modification of a previously described protocol (*9*). Briefly, after incubation at 37 °C, cells were washed twice and lysed by a mix of PBS and SDS 1% (w/v) in the presence of protease inhibitors. Nondegraded proteins were precipitated by adding TCA (6% (w/v) final concentration). After centrifugation, free iodine, present in the supernatant, was oxidized with potassium iodine (40%, p/v) and hydrogen peroxide, then extracted in the presence of chloroform. Degradation was determined by radioactivity measurement and expressed as nanograms of protein HDL degraded per dish (average cell number of 4×10^5).

Data Analysis. Binding and competition assays were analyzed using a weighted nonlinear curve-fitting program, based on the LIGAND analysis program (*10*). In competition experiments, the sigmoidal curves were transformed into a linear relationship, using the logit transformation (*11*). The data are represented in a logit-log(lipoproteins) plot. The IC_{50} (i.e., the concentration that inhibits 50% of the binding), which corresponds to a logit value of 0, was determined by linear regression analysis.

Analytical Procedures. The protein concentration was determined by the method of Bradford (*12*), using the Bio-Rad protein assay dye and bovine serum albumin (BSA) as a standard.

RESULTS

The saturation, kinetics, and competition experiments were performed at 4 °C in PBS with $HepG_2$ cell monolayers as previously described (*4*). A Scatchard representation of the binding of triglyceride rich HDL_2 and remnant HDL_2 on $HepG_2$ cells clearly shows two binding components for remnant HDL_2 (Figure 1) and HDL_2 (not shown), whereas triglyceride rich HDL_2 bind only the low-affinity sites. The calculated binding parameters from Figure 1 are represented in Table 1. The difference in the K_d value of remnant HDL_2 toward the low- and high-affinity binding sites (140-fold) was not great enough to allow us to follow the kinetics and competition parameters of the high-affinity binding sites, simply by using a low concentration of labeled remnant HDL_2.

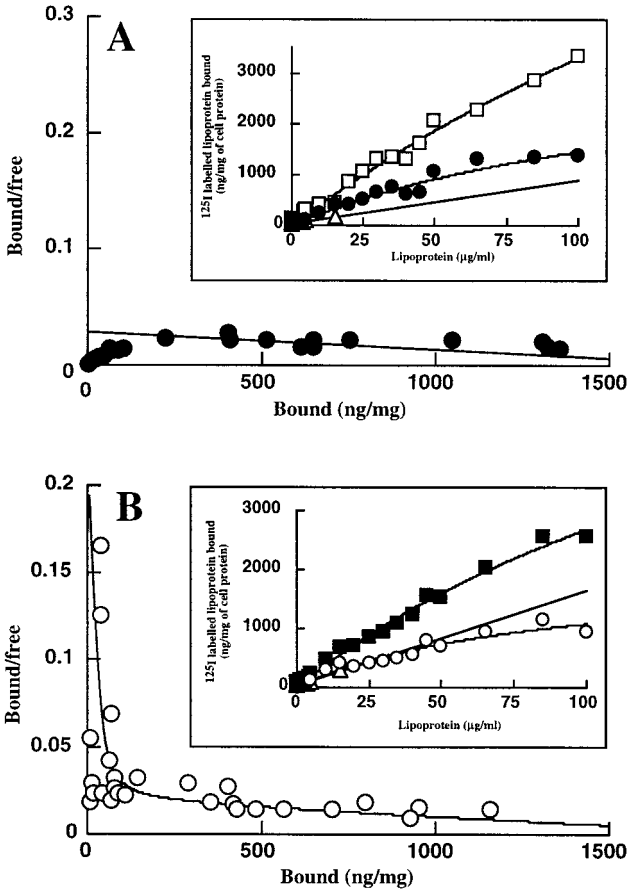

FIGURE 1: Scatchard representation and binding isotherm of ^{125}I-labeled triglyceride rich HDL_2 and ^{125}I-labeled remnant HDL_2 to $HepG_2$ cells. Specific binding of ^{125}I-labeled triglyceride rich HDL_2 (A) and ^{125}I-labeled remnant HDL_2 (B) was measured on duplicate wells after 90 min of incubation at 4 °C. Nonspecific binding was assessed as described in the Experimental Procedures and represents 30% of total binding. The mean values from duplicate wells are reported (±10% from the mean) and are representative of three independent experiments performed on three different series of cells. (Inset) Corresponding binding isotherm of ^{125}I-labeled triglyceride rich HDL_2 and ^{125}I-labeled remnant HDL_2: total binding [triglyceride rich HDL_2 (□) and remnant HDL_2 (■)], specific binding [triglyceride rich HDL_2 (●) and remnant HDL_2 (○)], nonspecific binding (△).

Table 1: Binding Parameters of ^{125}I-Labeled Triglyceride Rich HDL_2 and ^{125}I-Labeled Remnant HDL_2 to $HepG_2$ Cells[a]

	high affinity		low affinity	
	K_d (μg/mL)	B_{max} (ng/mg)	K_d (μg/mL)	B_{max} (ng/mg)
TG rich HDL_2			93.03	2753.74
remnant HDL_2	0.507	100	70.68	1993.21

[a] Data were obtained from Scatchard plots of Figure 1 and are representative of three independent experiments performed on three different series of cells.

Consequently, kinetic experiments of triglyceride rich HDL_2 and remnant HDL_2 (Figure 2) were performed using 75 μg/mL of each lipoprotein particles, and the measured parameters correspond to the contribution of both the high- and low-affinity binding sites (Figure 2 and Table 2). Calculation of the association and dissociation rate constants for triglyceride rich HDL_2 and remnant HDL_2 enable us to estimate the K_d values. This calculated K_d values were of the same order as the K_d values of the low-affinity binding

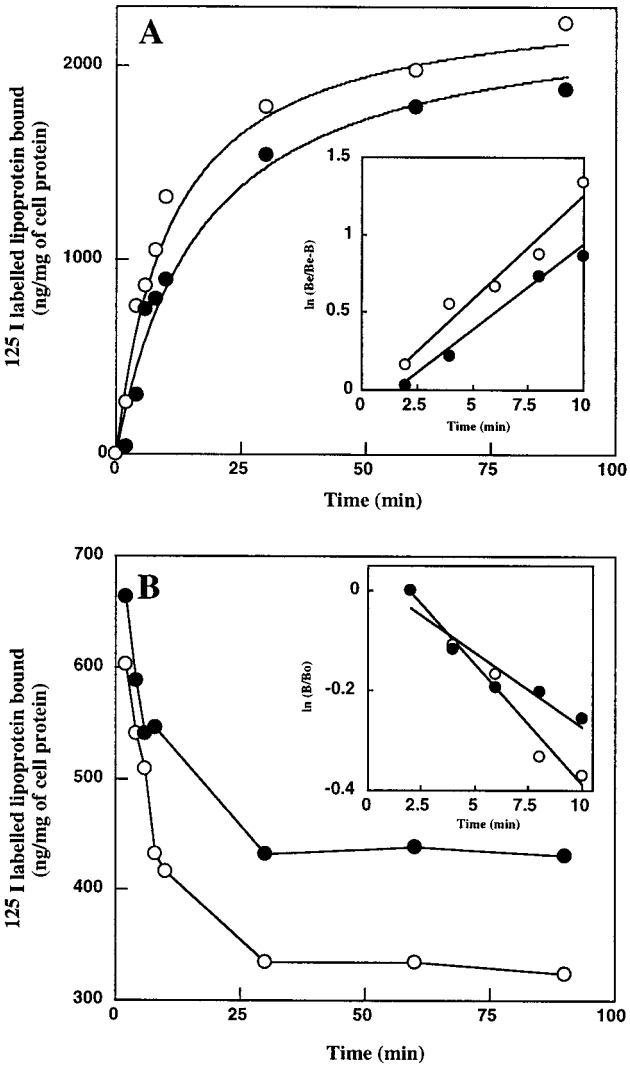

FIGURE 2: Kinetics of specific association and specific dissociation at 4 °C of ^{125}I-labeled triglyceride rich HDL_2 and ^{125}I-labeled remnant HDL_2 onto $HepG_2$ cells. A concentration of 75 μg/mL was used for specific association (A) and specific dissociation (B) of ^{125}I-labeled triglyceride rich HDL_2 (●) and ^{125}I-labeled remnant HDL_2 (○). A pseudo-first-order equation was used to calculate the association rate constant (k_{+1}) of the association. A plot of $\ln[B_e/(B_e - B_o)]$ versus time (A, right panel) enables calculation of the association rate constant as described in the Experimental Procedures. A first-order equation was used to calculate the dissociation rate constant (k_{-1}). As shown in the right panel B, a plot of $\ln(B/B_o)$ versus time has a slope of $k - 1$. The curves represent the specific binding calculated as described in the Experimental Procedures. Nonspecific binding averaged 40% of the total binding. The curves are representative of three experiments performed on three different series of cells.

Table 2: Kinetic Association and Dissociation of ^{125}I-Labeled Triglyceride Rich HDL_2 and ^{125}I-Labeled Remnant HDL_2 onto $HepG_2$ Cells[a]

	triglyceride rich HDL_2	remnant HDL_2
k_{-1} (min^{-1})	0.048	0.030
k_{+1} (min^{-1} $(mg/mL)^{-1}$)	0.818	1.4
K_d[b] (μg/mL)	58.8	21.21

[a] Data were obtained from Figure 2 and are representative of three experiments performed on three different series of cells. [b] Calculated $K_d = k_{-1}/k_{+1}$.

sites, as obtained from isotherm-binding experiments (Table 2). Furthermore, it is noteworthy that no significant differ-

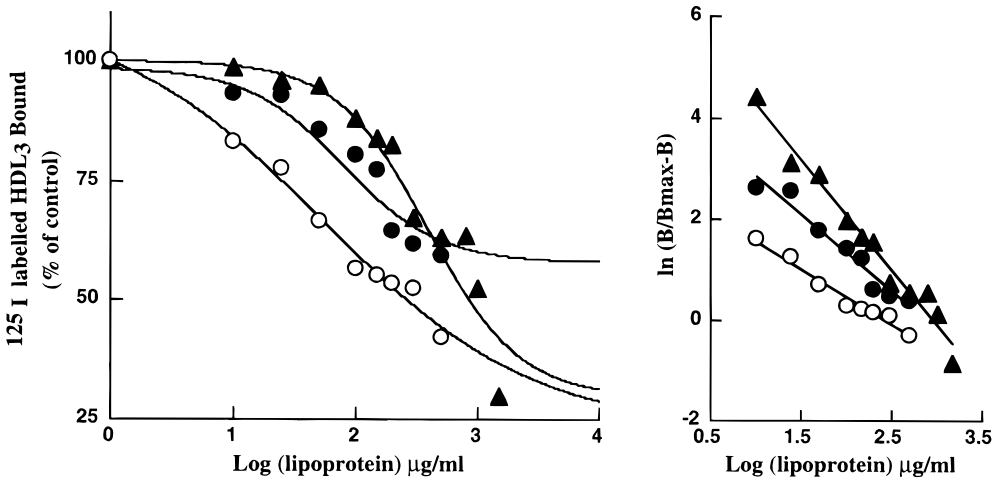

FIGURE 3: Competitive inhibition of the binding of ^{125}I-labeled HDL_3 to $HepG_2$ cells. $HepG_2$ cells were incubated for 90 min at 4 °C in the presence of 10 μg/mL ^{125}I-labeled HDL_3 and increasing concentrations of unlabeled HDL_3 (▲), triglyceride rich HDL_2 (●), and remnant HDL_2 (○). Nonspecific binding represented 30% of the total binding. (Right panel) A logit plot, as described in the Experimental Procedures, of each experiment is shown. One experiment representative of three independent experiments performed on three different series of cells.

ence was observed between the association and dissociation rate constants of triglyceride rich HDL_2 and remnant HDL_2.

To test whether the binding sites characterized for the triglyceride rich HDL_2 and remnant HDL_2 were the same as the binding sites already described for HDL_3 (*4*), we performed competition experiments with labeled HDL_3 (Figure 3). The data showed that both triglyceride rich HDL_2 and remnant HDL_2 particles are able to compete for the binding of labeled HDL_3, strongly suggesting that the binding sites for triglyceride rich HDL_2 and remnant HDL_2 were the same than those previously described for HDL_3 on $HepG_2$ cells. The slight difference observed (3.5-fold K_d^{app} difference) between triglyceride rich HDL_2 and remnant HDL_2 in competing with HDL_3 was not significant. It is noteworthy, that binding experiments performed in the presence of heparin (2 mg/mL) did not display any difference for triglyceride rich HDL_2 and remnant HDL_2, strongly suggesting that the binding observed was not dependent on the apoB/E receptor (data not shown). Furthermore, competition experiments performed using labeled free-apoA-I [which is specific of the high-affinity binding site (*4*)] clearly indicate that only remnant HDL_2 were able to compete for the high-affinity binding site (K_d^{app} = 5 μg/mL) whereas triglyceride rich HDL_2 were only poor competitors (K_d^{app} = not calculable).

We took advantage of the rapid dissociation of labeled triglyceride rich HDL_2 and remnant HDL_2 from their binding sites on $HepG_2$ cells (Figure 2) to assess the internalization of the triglyceride rich HDL_2 and remnant HDL_2 as described previously (*3*). Thus, at 4 °C, we were able to dissociate the ^{125}I-labeled triglyceride rich HDL_2 and ^{125}I-labeled remnant HDL_2 bound to the cell surface after a preincubation with $HepG_2$ cells at 37 °C and, thus, to precisely measure the internalization of triglyceride rich HDL_2 and remnant HDL_2 (Figure 4). As shown in Figure 4, the internalization of ^{125}I-labeled triglyceride rich HDL_2 and ^{125}I-labeled remnant HDL_2 into $HepG_2$ cells represents about 28 and 100%, respectively, of the total radioactivity measured at 37 °C. Kinetics of internalization and degradation of triglyceride rich HDL_2 and remnant HDL_2 were then measured at 37 °C for short (Figure 5, panels A and C) or long periods of times (Figure 5, panels B and D). Degradation of triglyceride rich

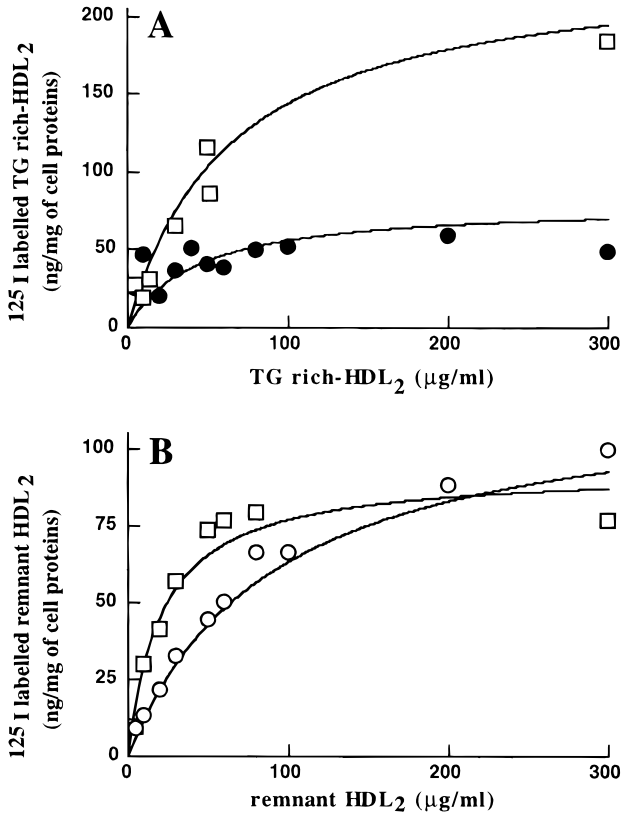

FIGURE 4: Internalization of ^{125}I-labeled triglyceride rich HDL_2 and ^{125}I-labeled remnant HDL_2 into $HepG_2$ cells. The sum of binding and internalization of ^{125}I-labeled triglyceride rich HDL_2 (A) and ^{125}I-labeled remnant HDL_2 (B) were measured on duplicate wells after 90 min of incubation at 37 °C (□). The following depletion of ^{125}I-labeled triglyceride rich HDL_2 (●) and ^{125}I-labeled remnant HDL_2 (○) bound on the cell surface was performed at 4 °C in the presence of PBS during 90 min and the remaining ^{125}I associated radioactivity was referred to as specific internalization. Nonspecific association and internalization was determined in the presence of an excess of nonlabeled HDL_3 as described in the Experimental Procedures. The mean values from duplicate wells are reported (±10% from the mean) and are representative of three independent experiments performed on three different series of cells.

HDL_2 and remnant HDL_2 was detected as the TCA-nonprecipitable material in cell lysates, and in long-time (over

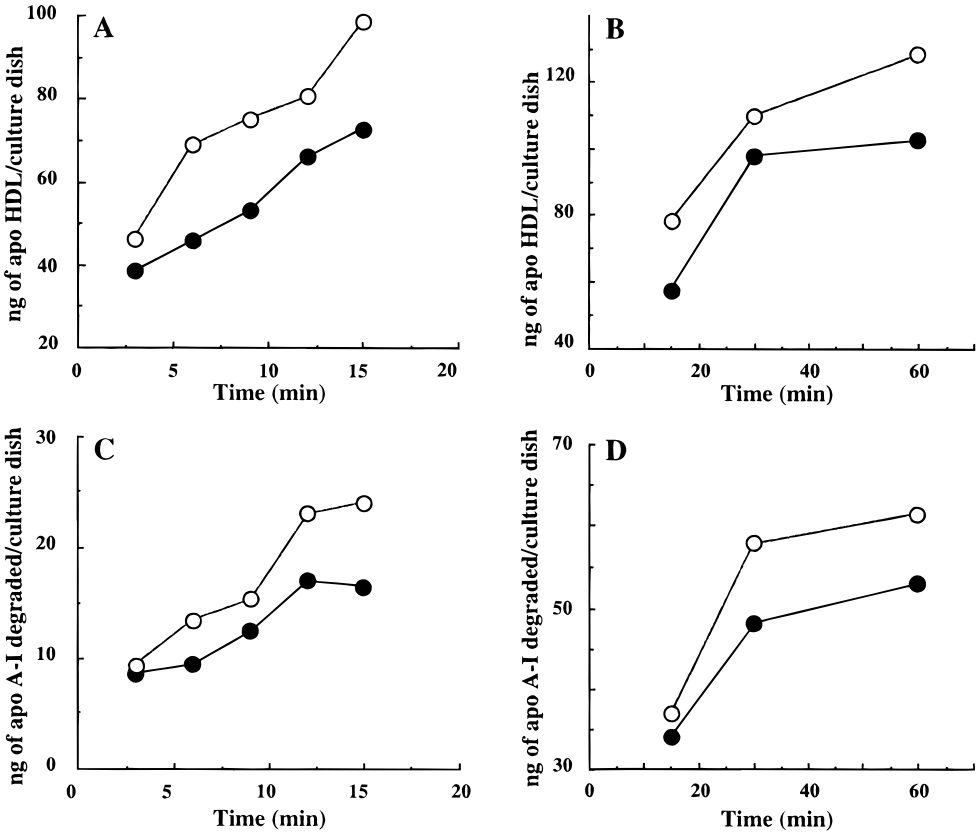

FIGURE 5: Kinetics of internalization and degradation of ^{125}I-labeled triglyceride rich HDL_2 and ^{125}I-labeled remnant HDL_2 onto $HepG_2$ cells. A concentration of 75 μg/mL was used for each experiment. Specific internalization (panels A and B) and specific degradation (panels C and D) of ^{125}I-labeled triglyceride rich HDL_2 (●) and ^{125}I-labeled remnant HDL_2 (○) were measured after 3, 6, 9, 12, and 15 min (panels A and C) or 15, 30, and 60 min (panels B and D) of incubation at 37 °C and 90 min of depletion with PBS at 4 °C. Specific degradation was assessed after internalization by measurement of the TCA nonprecipitable material present in the cells. The mean values from duplicate wells are reported (±10% from the mean) and are representative of four independent experiments performed on four different series of cells.

15 min) experiments. It represented 54 and 49%, respectively, of the corresponding lipoprotein particle internalizations. For shorter time kinetics (under 15 min), we measured a degradation rate of triglyceride rich HDL_2 and remnant HDL_2 of about 23 and 24%, respectively. The internalization and degradation of remnant HDL_2 as compared to triglyceride rich HDL_2 display a slight but very reproducible increase of 27 and 18%, respectively, for long incubation times, and 38 and 46%, respectively, for short time kinetics.

DISCUSSION

In the present study, we have characterized the interaction between the human hepatoma cell line $HepG_2$, triglyceride rich HDL_2, and remnant HDL_2, respectively. For this purpose, we took advantage of our previous knowledge of the HDL_3 interactions with $HepG_2$ cells (*3*, *4*), i.e., internalization and binding processes.

The first main observation was that remnant HDL_2, like HDL_3 (*4*), were able to bind to two classes of binding sites, in contrast with the parental lipoprotein triglyceride rich HDL_2. Furthermore, competition experiments indicate, first, that these two remnant HDL_2 binding sites were the same as the two HDL_3 binding sites previously described (*4*) on these cells. Second, using labeled free-apoA-I (which only bind to the HDL_3 high-affinity binding site), only remnant HDL_2s were able to compete for the high-affinity binding site as compare to the native triglyceride rich HDL_2. Altogether, these data clearly indicate that, in opposition to native triglyceride rich HDL_2, only the remnant HDL_2s, were able to bind the high-affinity binding sites on $HepG_2$ cells.

Previously, we had demonstrated that the binding of HDL_3 did not implicate the putative HDL receptor named scavenger receptor type BI (SR-BI) previously characterized by Acton et al. (*13*). Consequently, when we consider the competition experiments, it seems highly unlikely that the binding of triglyceride rich HDL_2 and remnant HDL_2 involves the SR-BI. Furthermore, the SR-BI does not promote HDL internalization when overexpressed in different cell systems (*13*). On the opposite, the triglyceride rich HDL_2 and remnant HDL_2 particles were internalized by $HepG_2$ cells, suggesting again that this process does not involve SR-BI. Recently, a human receptor, named CLA-1, analogous to the CD36, LIMPII, and SR-BI receptor class, was described as a potential high-affinity receptor for VLDL, LDL, oxLDL, acLDL, and HDL (*14*). The HDL affinity described for CLA-1 ($K_d = 2$ μg/mL) is very comparable with the K_d value we observed for the remnant HDL_2 and HDL_3 high-affinity binding sites, suggesting that the high-affinity binding site onto $HepG_2$ cells could involve CLA-1. But, on the opposite, the broad range of ligands observed for CLA-1 by the authors is very different compared to the narrower ligand specificity for $HepG_2$ high-affinity binding sites (*4*), suggesting that this high-affinity binding site would also be different from CLA-1. Finally, another candidate to putative HDL liver receptors

was proposed. Indeed, Hidaka et al. (*15*) have identified two liver plasma membrane proteins named HB1 and HB2 (for HDL-binding protein 1 and 2) which are candidate HDL receptors, and more recently, the HB2 cloning and characterization was realized (*16*). Thus, in the present study, we cannot completely exclude the possibility that the HDL binding we observed on $HepG_2$ cells involved the HB1 or/and the HB2.

The size, the molecular lipid composition, and the physical characteristics of triglyceride rich HDL_2 and remnant HDL_2 particles are different (article under publication) and this may result in a different apolipoprotein conformation. This conformation change could mask or unmask some apolipoprotein domains and thus explain the ability of remnant HDL_2 to bind to the high-affinity binding site. One way to detect these modifications of domain exposure could be, for instance, the use of monoclonal antibodies specific of defined apolipoprotein epitopes (work in progress) as developed in several laboratories (*17*).

To confirm our hypothesis that the triglyceride rich HDL_2 and remnant HDL_2 binding differences are reflected in the metabolic behavior of these particles, we performed internalization studies. Interestingly, while around 50% of the pre-bound triglyceride rich HDL_2 was internalized in agreement with the data for HDL_3 (*3*), a proportion of 100% was measured with remnant HDL_2, strongly suggesting that the binding to the high-affinity binding site might enhance the remnant HDL_2 internalization. An alternate explanation would be that both kind of particles can undergo internalization in comparable amounts, but that the membrane associated particles following a 37 °C incubation would be almost undetectable in the case of remnant HDL_2. This means that, in contrast with triglyceride rich HDL_2, receptor sites would not be able to bind further remnant HDL_2 particles after the internalization had occurred, suggesting a different routing for the internalized remnant HDL_2. The main receptor-dependent internalization route demonstrated so far is the clathrin-coated vesicles pathway. In this process, the ligands and the receptors are cointernalized through the clathrin-coated vesicles and then the receptors are either degraded with the ligand (see, for review, ref *18*) or recycled to the cell surface as it was described for the LDL internalization. In the first case, the cell surface number of receptors either goes down or remains constant due to the presence of new receptor molecules to the cell surface. In the case of triglyceride rich HDL_2 versus remnant HDL_2 internalization, one hypothesis could be that, in the receptor cycle, the receptor retroendocytosis pathway is interrupted in the case of the remnant HDL_2 used as a ligand. If this hypothesis was verified, it would be the first evidence that a simple conformational change of a ligand could trigger a different cellular routing of a cell surface receptor. Of course, the mechanisms of such processes remain unknown today and need to be further investigated. We have previously demonstrated that HDL_3 were internalized in $HepG_2$ cells by a mechanism involving the formation of clathrin vesicles, and we would like to suggest that the same process occurred in the case of other HDL particles (*3*). We demonstrated also at this time, that the major part of HDL_3 internalization occurred through the low-affinity binding site. Following our hypothesis, the high-affinity binding site for remnant HDL_2 could trigger internalization through the low-affinity one and then could explain the internalization difference between triglyceride rich HDL_2 and remnant HDL_2. Furthermore, this difference is also evident in internalization and degradation kinetic experiments where the remnant HDL_2 were internalized and degraded in all cases faster and in higher amounts than triglyceride rich HDL_2. This difference was more important for the short periods of time, suggesting that, in cell culture, endocytosis was a saturable process. Interestingly, this observation could explain why, in concentration-dependent experiments, the triglyceride rich HDL_2 and remnant HDL_2 reach the same internalization plateau. Altogether, these observations represent the first potential role ever described today for this new high-affinity binding site.

Increased HDL concentrations are classically accepted to be protective against the development of atherosclerosis and coronary artery disease, but recent observations have indicated that the underlying cause of this increased HDL may affect whether it is protective or detrimental depending which HDL particle increases (*19*). Thus, the dynamics of cholesterol transport through HDL (i.e., reverse cholesterol transport) need to be associated with HDL concentration to determine the antiatherogenicity of the HDL fraction (*20*). A fully active hepatic lipase (HL), due to its pivotal position downstream of the reverse cholesterol transport, could be a critical step for the homeostasis of this dynamic cholesterol transport. Thus, synergistic effects of hepatic lipase with other active proteins in the reverse cholesterol transport (like cholesterol ester transfer protein), on the HDL remodeling, have been extensively studied in vitro and represent an essential step in the cholesterol removal by the liver (*21*). This work helps to understand the mechanism by which hepatic lipase participates in the removal of these HDL since after lipolysis we showed that HDL_2 are removed more rapidly by rat liver (*5*). The mechanism by which these particles are removed is not yet well defined. Nevertheless, we suggest that hepatic lipase inducing a major remodeling of HDL particles generates remnant HDL particles which display high-affinity binding and accelerated processing in liver cells. This new observation enlightens the importance of studies of a well-defined HDL particle which could interact with a particular tissue or cell type.

REFERENCES

1. Miller, G. J., and Miller, N. G. (1975) *Lancet 1*, 16−19.
2. Eisenberg, S. (1984) *J. Lipid Res. 25*, 1017−1058.
3. Garcia, A., Barbaras, R., Collet, X., Bogyo, A., Chap, H., and Perret, B. (1996) *Biochemistry 35*, 13064−13070.
4. Barbaras, R., Collet, X., Chap, H., and Perret, B. (1994) *Biochemistry 33*, 2335−2340.
5. Barrans, A., Collet, X., Barbaras, R., Jaspard, B., Manent, J., Vieu, C., Chap, H., and Perret, B. (1994) *J. Biol. Chem. 269*, 11572−11577.
6. Sinn, H. J., Schrenk, H. H., Friedrich, E. A., Via, D. P., and Dresel, H. A. (1988) *Anal. Biochem. 170*, 186−192.
7. Scatchard, G. (1949) *Ann. N. Y. Acad. Sci. 51*, 660−672.
8. Bylund, D. (1980) in *Receptor binding techniques*, pp 70−99, Cincinnati Society for Neuroscience.
9. Brown, M. S., Faust, J. R., and Goldstein, J. L. (1975) *J Clin. Invest. 55* (4), 783−93.
10. Munson, P. J., and Rodbard, D. (1980) *Anal. Biochem. 107*, 220−239.
11. Rodbard, D., and Frasier, G. R. (1975) *Anal. Biochem. 20*, 525−532.
12. Bradford, M. (1976) *Anal. Biochem. 72*, 248.

13. Acton, S., Rigotti, A., Landschulz, K. T., Xu, S., Hobbs, H. H., and Krieger, M. (1996) *Science 271*, 518−520.
14. Calvo, D., Gomez-Coronado, D., Lasuncion, M. A., and Vega, M. A. (1997) *Arterioscler. Thromb. Vasc. Biol. 17*, 2341−2349.
15. Hidaka, H., and Fidge, N. H. (1992) *Biochem. J. 284*, 161−167.
16. Matsumoto, A., Mitchell, A., Kurata, H., Pyle, L., Kondo, K., Itakura, H., and Fidge, N. (1997) *J. Biol. Chem. 272* (27), 16778−16782.
17. Leblond, L., and Marcel, Y. L. (1993) *J. Biol. Chem. 268* (3), 1670−1676.
18. Goldstein, J. L., Brown, M. S., Anderson, R. G. W., Russell, D. W., and Schneider, W. J. (1985) *Annu. Rev. Cell Biol. 1*, 1−39.
19. Hill, S. A., and McQueen, M. J. (1997) *Clin. Biochem. 30* (7), 517−525.
20. Hill, S. A., Nazir, D. J., Jayaratne, P., Bamford, K. S., and McQueen, M. J. (1997) *Clin. Biochem. 30* (5), 413−418.
21. Bruce, C., and Tall, A. R. (1995) *Curr. Opin. Lipidol. 6* (5), 306−311.

BI9810508